Li, B., Li, J., Huang, Y., Yin, H., Lin, C.-H., Wei, D., Shen, X., Liu, J., and Chen, Q. 2016. "Experimental studies of thermal environment and contaminant transport in a commercial aircraft cabin with gaspers on," *Indoor Air*, 26: 806-819

# Experimental studies of thermal environment and contaminant transport in a commercial aircraft cabin with gaspers on

Bingye Li[1], Jianmin Li[1], Yan Huang[1], Haishen Yin[1], Chao-Hsin Lin[2], Daniel Wei[3], Xiong Shen[1,*], Junjie Liu[1], and Qingyan Chen[1,4]

[1]Tianjin Key Laboratory of Indoor Air Environmental Quality Control, School of Environmental Science and Engineering, Tianjin University, Tianjin 300072, China

[2]Environmental Control Systems, Boeing Commercial Airplanes, Everett, WA 98203, USA

[3]Boeing Research & Technology, Beijing 100027, China

[4]School of Mechanical Engineering, Purdue University, West Lafayette, IN 47907, USA

[*]Email address: shenxiong@tju.edu.cn

## Abstract

Gaspers installed in commercial airliner cabins are used to improve passengers' thermal comfort. To understand the impact of gasper airflow on the air quality in a cabin, this investigation measured the distributions of air velocity, air temperature, and gaseous contaminant concentration in five rows of the economy-class section of an MD-82 commercial aircraft. The gaseous contaminant was simulated by using $SF_6$ as a tracer gas with the source located at the mouth of a seated manikin close to the aisle. Two fifths of the gaspers next to the aisle were turned on in the cabin, and each of them supplied air at a flow rate of 0.66 L/s. The airflow rate in the economy-class cabin was controlled at 10 L/s per passenger. Data obtained in a previous study of the cabin with all gaspers turned off was used for comparison. The results show that the jets from the gaspers had a substantial impact on the air velocity and contaminant transport in the cabin. The air velocity in the cabin was higher, and the air temperature slightly more uniform, when the gaspers were on than when they were off, but turning on the gaspers may not have improved the air quality.

**Keywords:** Air velocity, air temperature, gaseous contaminant concentration, measurements, jets, gaspers

## Practical implications

This study has provided a set of accurate experimental data on the distributions of air velocity, air temperature, and gaseous contaminant concentration in a commercial aircraft cabin.

## Introduction

An airliner cabin has a very high population density (Wisthaler et al., 2007), a low outside airflow rate (Haghighat et al., 1999), and multiple heat sources. Therefore, the design of systems to ensure thermal comfort and good air quality in the cabin is very challenging. The environmental control system (ECS) for an aircraft cabin supplies air through inlets in the upper part of the cabin and exhausts the air through the sidewalls near floor level, which causes the mixing of air in the cabin. A number of studies have addressed the air distribution in a cabin mockup (Zhang et al., 2009; Kühn et al., 2009; Wang et al., 2008; Lin et al., 2006; Yan et al., 2009) and on an airplane (Liu et al., 2012; Bosbach et al., 2006; Li et al., 2014). The studies have shown that the air velocity in a cabin tends to be low, while the turbulent intensity is high, and the air temperature tends to be uniform. Passengers have different requirements in regard to thermal environmental conditions, and they can use overhead gaspers to increase air circulation if they feel too warm or cover themselves with blankets if they feel too cold. When a gasper is turned on, its high-velocity jet affects the thermal environment and air quality not only for the passenger immediately below the gasper, but also for surrounding passengers.

Several studies conducted in buildings have shown that personalized ventilation devices can improve not only thermal comfort but also local air quality (Melikov et al., 2002; Li et al., 2010). When Niu et al. (2007) studied a chair-based personalized ventilation system, however, they found that although it greatly improved air quality in the breathing zone, discomfort was caused by the high air speed in the head region. Regarding the gaspers in aircraft cabin, Dai et al. (2014) studied the flow characteristic at the gasper inlet. They did not investigate the effect of the jet flow on the cabin air distribution. Anderson (2010) applied carbon dioxide as tracer gas to investigate the effect of gaspers on the transmission of airborne contaminants in a Boeing 767 aircraft cabin mockup. Since they did not measure the airflow distributions in the cabin, it was difficult to explain the influence of gasper inlet on the contaminant transmission. The previous studies show that the impact of gasper performance on thermal comfort and air quality in aircraft cabins remains unknown. Therefore it is important to conduct such an investigation. The objective of our study was to measure the distributions of air velocity, air temperature, and contaminant concentrations in an aircraft cabin with a portion of the gaspers turned on. This information can then be used to assess the impact of gasper operation on thermal comfort and air quality.

## Method

### Description of the research facility

The air environment research facility used in this study was the cabin of an MD-82 airplane parked on the ground at Tianjin University in China, as shown in Figure 1(a). Our experiment was conducted in a section of the economy-class cabin from row 7 to row 11, as shown in Figure 1(b) and (c). We observed an obvious longitudinal flow, and the cabin was partitioned between rows 3 and 4 and between rows 13 and 14 to minimize this flow. This left ten rows of

seats in the section of the cabin. Rows 4, 5 and 13 were empty seats and rows 6 to 12 (seven rows) were occupied with heated manikins. As shown in Figure 1(b), each row had manikins. Each of the heated manikins had a power input of 75 W, which is the typical sensible heat released by a passenger. Figure 1(d) shows the sketch of the cabin cross-section with enlarged gasper location and direction. The air inlets were located on the upper part of the side walls and the outlets were at the bottom of the cabin. Among the five gaspers in a row, this study turned on the gaspers for seat B and C because our observation found that up to two gaspers were opened in airline normal operation.

The HVAC system was the same as the one applied in the study by Liu et al. (2012). In the experiment, the air recycling system in the aircraft was turned off. A ground air-conditioning cart was used to supply air to the cabin through sidewall diffusers, which are part of the general air distribution system. The air was exhausted through the sidewalls at floor level. The airflow rate in the economy-class cabin was controlled at 10 L/s per passenger, which is typical for commercial airplanes as recommended by ASHRAE Standard 161 (2007). This investigation also measured the ventilation rate in the ten-row cabin (rows 4-13) to be 1210 $m^3$/h, among which only 52 $m^{3/}$h was from the gaspers. The air supply temperature was maintained at 20±1 ºC.

(a)

(b)

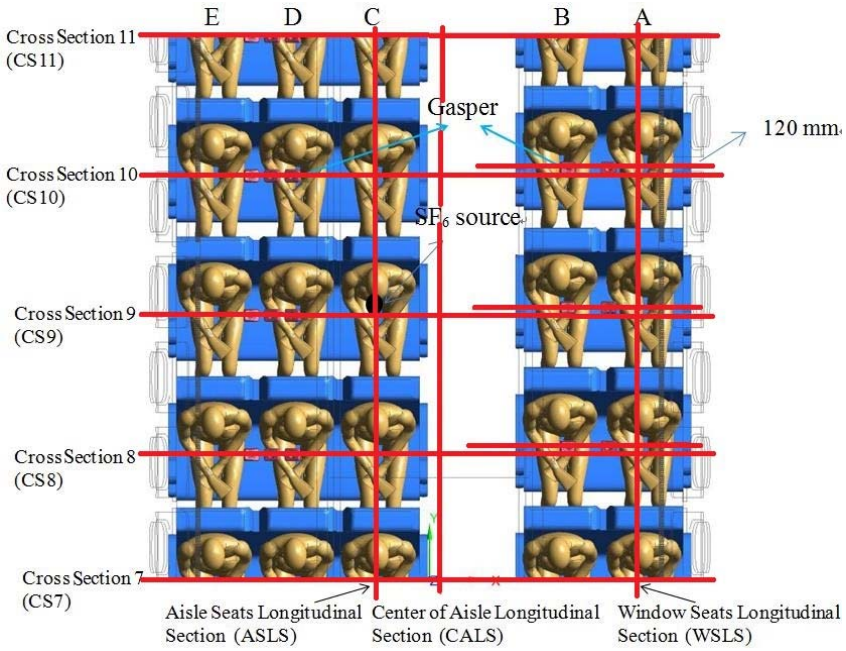


(c)

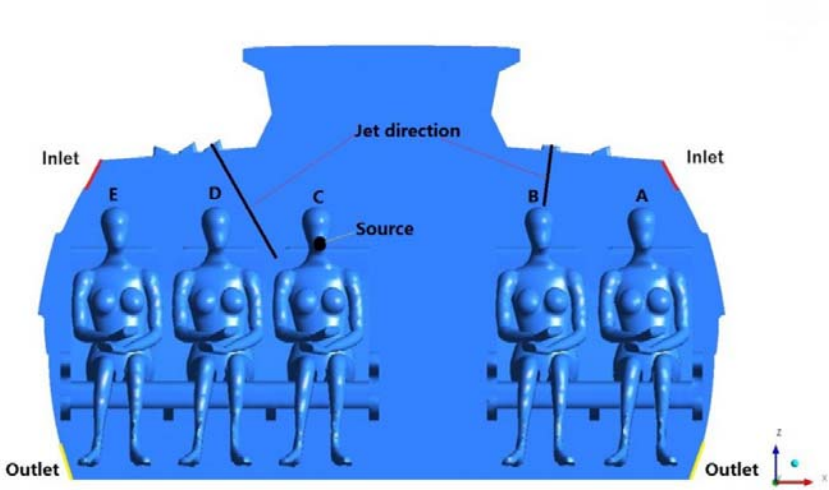


(d)

*Figure 1. Air environment research facility at Tianjin University in China: (a) MD-82 plane with insulated fuselage, (b) interior of the economy-class cabin with heated manikins, (c) the cabin section that was studied (rows 7 to 11), and (d) locations of the main air diffuser inlets and return outlets and the locations and air supply directions of two opened gaspers for passengers B and C.*

## Control of the thermal-fluid boundary conditions inside the cabin

When the aircraft was directly exposed to the outside environment, solar radiation and temperature changes had a major impact on the interior environment of the cabin. To ensure stable thermal boundary conditions for the cabin, the aircraft fuselage was insulated with double layers of closed-cell sponge rubber material, as shown in Figure 1(a). Each layer was 0.03 m thick, and the total thermal conductivity was 0.032 W/(m·K). With the original insulation of the airplane and the new added insulation, the heat transfer through the walls was minimal. Figure 2 depicts the temperature changes at the interior wall surfaces when insulation was present, during our experimental period of September 27, 2013, to May 29, 2014. Throughout the experiment, the temperature at the inner sidewall surface was maintained at 25.1±1.8 ºC that was very stable and was similar to that reported by Zhang, et al. (2012). The temperature of the floor surface at 23.0±3.1 ºC. The insulation helped to maintain stable interior surface temperatures.

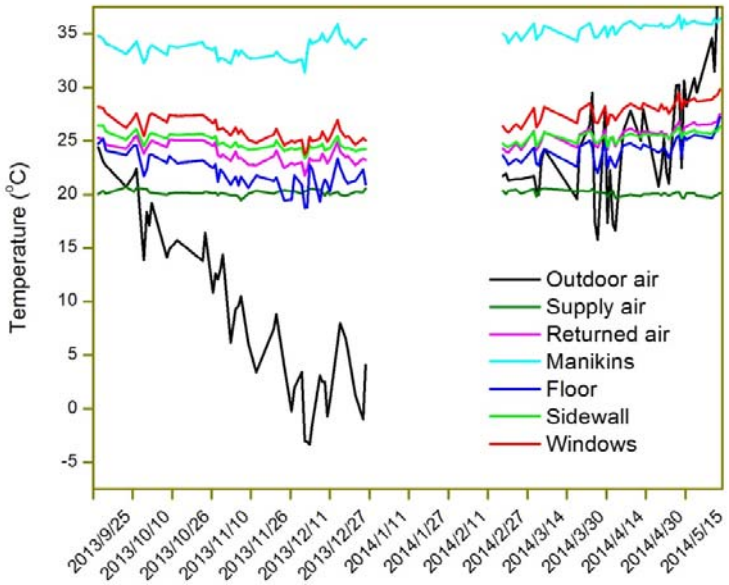


*Figure 2. Temperature variations of the interior surfaces of the cabin and the outdoor air during the experimental period of September 27, 2013, to May 29, 2014.*

Because of safety and noise-control regulations, our experiment could be conducted only between 8:00 and 17:00 from Monday through Friday. On a typical day during the experiment, the supplied air temperature became stable very quickly, but it took four hours to heat the manikins to a stable condition, as shown in Figure 3. Thus, a very long preparation time was required each day before the measurements could be conducted. This requirement was the reason for the experiment's overall duration of approximately half a year. During the experiment, thermal conditions were monitored at the wall surfaces, manikins, and air diffuser inlets and outlets. At stable conditions, the temperature of the supplied air was 20.1±0.2 ºC; the surface temperature of the manikins, which was measured at mid-chest level where the heat flux was high, was 34.5±1.5 ºC; and the temperature of the returned air was 25ºC±1.2 ºC. Measurements of airflow, temperature, and contaminant concentration fields were conducted after the thermal boundary had become stable. A robot system was used to move the sensors

during the measurements.

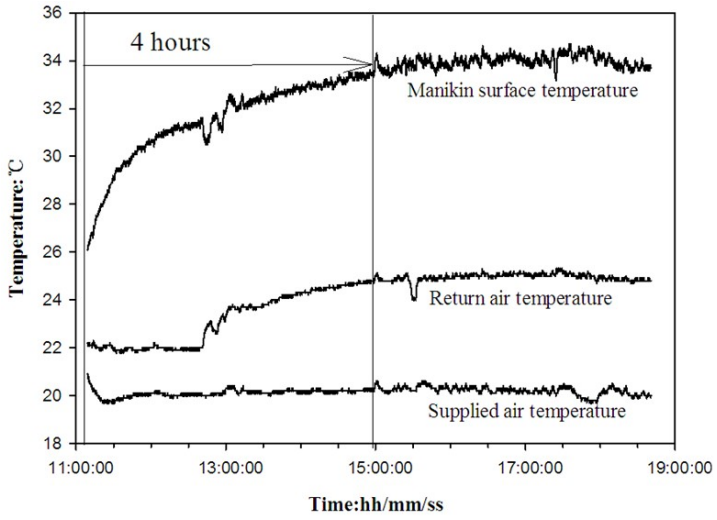


*Figure 3. Temperature variations on a typical day after the ground air-conditioning cart was turned on and the manikins were heated.*

**Measurements of gasper boundary conditions**

The aircraft is equipped with one overhead gasper per passenger, and the gaspers for a given row are grouped on each side of the aisle, as shown in Figure 4(a). The size of the gasper opening and the direction of the jet are adjustable to meet the individual needs of passengers. The airflow rate can be adjusted from 0 to 1.5 L/s per gasper but this experiment set the airflow rate to be 0.66 L/s. The gaspers on this airplane supply air through an annular region, as shown in the schematic in Figure 4(b). The diameter of the annular nozzle opening of the gasper was 20 mm, and inside the opening there was a conical structure. The locations of the gaspers in the cabin are indicated by the red squares in Figure 1(c). The locations of the gaspers relative to the seats are the same for all rows of the economy-class cabin. In practice, not all passengers turn on their gaspers. In this experiment, the gaspers were turned on only for the manikins in the B and C seats in Figure 1(d). Thus, among the 10 rows with 50 gaspers, only 20 of them were turned on. The flow direction of each of the opened gaspers was adjusted towards the manikins on seats B and C as shown by the red lines in Figure 1(d).


(a) (b)

*Figure 4. The gaspers installed in the aircraft: (a) three gaspers grouped for passengers in the C, D, and E seats and (b) schematic diagram of the center section of the gasper.*

In the study, we set the airflow rate at the gaspers according to comfort level of seated passengers. ASHRAE Standard 161 (2007) stipulates that in the head region of a passenger, the air velocity should be in the range of 1 to 3 m/s when the gasper is turned on. On the basis of this standard, we adjusted the gaspers in the ten-row cabin to ensure that the velocity was within this range at head level. The velocity was within this range when the distance between the conical structure and annular opening (determined by rotating the knob) was between 0.89 and 1.45 mm, with an average of 1.2 mm. Consequently, a medium value of airflow rate (0.66 L/s) was set at the gaspers.

When measuring the flow rate through the gaspers, we applied the constant concentration tracer-gas method (Chao et al., 2004; Etheridge and Sandberg, 1996). Sulfur-hexafluoride ($SF_6$) was used as the tracer gas. Figure 5 shows the setup for measuring the flow rate. The tracer gas was injected into a transparent tube underneath the gasper. The concentration of $SF_6$ was measured at five positions at the bottom of the tube. The concentration was found to be $2.5\times10^5$ ppm at the center of the outlet and 1.5-2% lower at the other four positions which indicated that there were no substantial differences in $SF_6$ concentration at the five positions. The flow rate through the gasper was equal to the $SF_6$ flow rate divided by the $SF_6$ concentration at the tube outlet. The measurements were conducted twice to ensure their repeatability. The differences between two measurements ranged from 0% to 7%. The flow rates from 20 opened gaspers in the ten-row economy-class cabin were measured, and the flow rate for each of the gaspers was 0.66±0.03 L/s. At this flow rate, the air velocity in the head region of the manikin was 1.29±0.15 m/s. The differences between gaspers were small.

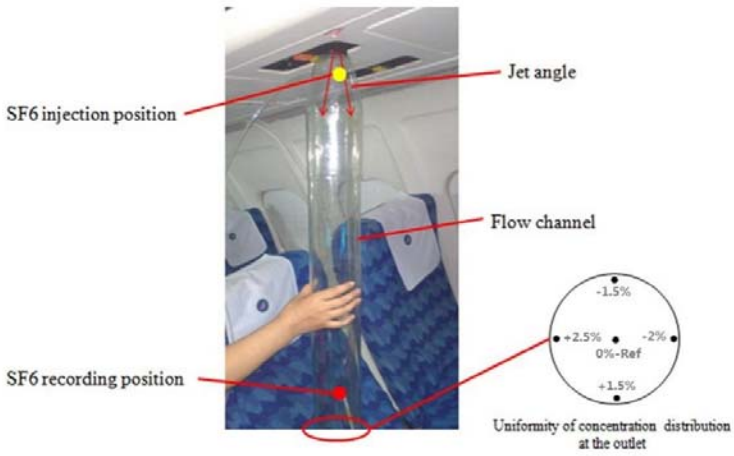


*Figure 5. Measurement of flow rate through a gasper.*

For accurate measurement of the airflow boundary at the gaspers, it was essential to position the measuring probes precisely because of the small dimensions of the gasper openings. In this context, we used a three-dimensional robot system to position the probe as shown in Figure 6. The system had a high positioning resolution of 0.01 mm, and the coordinates could be programmed into the system in order to achieve automatic motion. To measure the gasper inlet air velocity, our investigation used a hot-wire anemometer (HWA) with a measuring range of 0 to 70 m/s and a frequency of up to 105 Hz, as shown in Figure 6. Air velocity and turbulence were measured in two mutually perpendicular directions away from the gaspers. The measuring time at each position was 20 seconds.

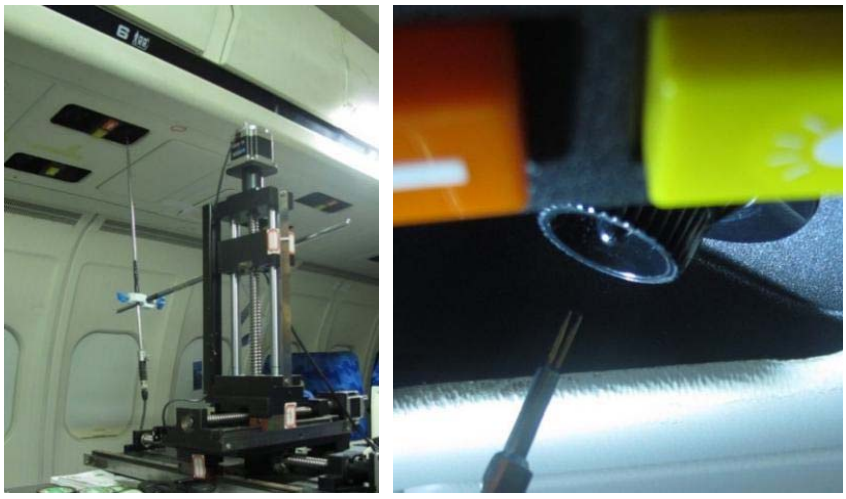

*(a)* *(b)*

*Figure 6. Placement of a hot-wire anemometer close to a gasper in the economy-class cabin: (a) the robot system and (b) the hot-wire probe.*

**Measurements of the air distributions in the cabin**

To investigate the air distributions in the cabin with gaspers turned on, this investigation measured the distributions of air velocity, air temperature, and concentration of a contaminant simulated by $SF_6$. Figure 1(c) shows the positions of the five measured cross sections (those at row 7 (CS7), row 8 (CS8), row 9 (CS9), row 10 (CS10), and row 11 (CS11)) and three longitudinal sections (through the aisle seats (ASLS), through the center of the cabin (CALS), and through the window seats (WSLS)).

The air velocity distributions were measured by seven Kaijo ultrasonic anemometers (Model DA-650) with TR-92T probes. The TR-92T anemometer probe has a span size of only 3 cm, so the error was small. The anemometers can measure air velocity between 0 and 10 m/s with 1% accuracy and 0.005 m/s resolution. The sampling frequency was 20 Hz, and the measuring time at one position was ten minutes, which reduced the measuring error to less than 0.005 m/s. As the anemometers measured the averaged velocity within its 6 heads enclosed a volume 3 cm x 3 cm x 3 cm, it would not measure accurately when the velocity gradient is large as one may find in some areas of this study.

The air temperature fields were measured by thermocouples with a precision of ±0.5 K. The measurement time for temperature at each sampling point was also ten minutes, but the measuring frequency was 1 Hz.

The contaminant concentration field measurements used a tracer gas that was a mixture of 1% $SF_6$ and 99% $N_2$ to simulate a gaseous contaminant exhaled by a passenger. In this study, the breathing was not simulated with a constant release of tracer gas from the source. This would have impact in the limited area around the passenger. Because the density of the $SF_6$-$N_2$ mixture is similar to that of air, the buoyancy effect could be neglected. The $SF_6$ concentration was analyzed with a photo-acoustic multi-gas analyzer (INNOVA Model 1309). During the measurements, the tracer gas was released continuously from a porous rubber bulb mounted in the mouth of a seated manikin. The total volume flow rate of the gas mixture released from the bulb was only 1 L/min, at which rate there is no observable air movement on the bulb surface. The tracer-gas source can be considered as having zero momentum. Details of the setup for $SF_6$ measurements have been described by Li et al (2014). We found that the $SF_6$ concentration needed to be measured for at least eight minutes at each position in order to obtain a mean concentration. According to Li et al. (2014), the corresponding error in measuring $SF_6$ would be less than 14%. Since we simultaneously measured air velocity, air temperature, and $SF_6$ concentration, the total measurement time was set as ten minutes at each position.

Figure 7 shows another three-dimensional robot system that was used to measure the air distributions in the cabin. Three types of sensors were mounted on this system: ultrasonic anemometers, thermocouples, and tracer-gas sampling tubes. The movement resolution of the

robot in the three directions was ±0.5 mm. The minimum traveling speed of the robot was 5 mm/s. The three-dimensional system was composed of X, Y, and Z direction manipulators, which were fixed on the floor of the aisle in order to move the instruments in the cross-sectional, longitudinal, and vertical directions of the cabin, respectively. The instrumentation platform was located on a sliding piece of the X-direction manipulator for positioning of the sensors. Moving the sensors from one position to another may have disturbed the air distribution in the cabin. Therefore, after moving the sensors we wait for one minute to ensure that the flow had stabilized before starting the measurement. This time period was sufficient because the three-dimensional robot system traveled at a very slow speed of 10 mm/s.


*Figure 7 Setup of the sensor probes on the 3D robot system for measurements at a cross-section*

The air distribution measurements were conducted with a uniform sampling resolution of 0.12 m in width and 0.12 m in height for the cross and longitudinal sections. The sampling at the bottom was 0.12 m above the floor and at the top was 0.12 m below the ceiling. Eight sampling points were uniformly distributed with a width of 0.2 m below the chairs in the longitudinal and cross sections, respectively. Because the robot cannot place the sensors in that region, the measurement in those locations was manually operated. These sections were selected so that detailed data could be obtained on the airflow characteristics in the cabin. There were a total of 744 sampling locations in the three longitudinal sections and 1100 in the five cross sections.

Our previous study (Liu et al., 2012) measured the air distributions in the cabin when all the gaspers were off. The data from that study has been used for comparison with the data obtained in the present investigation, where two fifths of the gaspers were turned on. Our previous study had a measuring resolution of 0.10 m by 0.10 m in the cross sections, and a resolution of 0.10 m along the height and 0.20 m along the length of the longitudinal sections. Fewer sampling points were used in that study than in the current study. Furthermore, because

the air distribution measurements in our previous study were conducted without the robot system, the errors may have been much higher.

The distribution of sampling points would lead to error of the temperature and concentration field measurement. This was because based on the theory by Huang et al. (2014), the region with large gradient should apply more sampling points than other regions, for example, at the gasper jet flow region. However, Li et al. (2014) compared the cases with more sampling points added into the field region with large gradients, the results shows no significant difference between cases. Thus, the distribution of samplings in this study was appropriate.

## Results

### Air velocity and temperature distributions with gaspers off and on

Figure 8 compares the distributions of air velocity and temperature in the five cross sections of the occupied economy-class cabin with the gaspers off and on. When the gaspers were off, the regions with high air velocity were created by the jets from the main diffusers (in Figure 1(d)). This jet momentum was the primary driving force of air movement in the cabin. When the gaspers above seats B and C were on, the jets from the gaspers penetrated the thermal plumes formed by the heated manikins. The jets from the diffusers and those from the gaspers merged in the aisle. The air velocity in the cabin was higher when the gaspers were on. The recirculation of air became more evident, with low velocities in the recirculation zone. Thus, the impact of gasper operation on the air distribution was obviously seen in the cross-sections especially in CS8 and CS9, although the flow rate was not high.

The measured cross-section was offset from seats D and E by nearly 120 mm. This is the reason why strong jets from the gaspers can be seen at cross-sections CS8, CS9, CS10 and CS11 in Figure 8. This study tried to maintain the same flow rate at all of the gaspers that were turned on, but the jet direction may have varied from gasper to gasper. Because of the complexity of the velocity profile at the diffusers and uncertainties in the airflow from the gaspers, the global airflow patterns and the local velocities in different sections were not identical.

The air temperature distributions in the occupied cabin were affected by the heat generated by the manikins. The thermal plumes from the manikins enhanced the mixing of air and reduced the air temperature stratification. Because the diffusers and gaspers supplied cool air to the cabin, the temperature in the region downstream from a jet was lower than the mean air temperature in the cabin. Overall, because the thermal plumes from the heated manikins mixed with the cool jets, the temperature in the cabin was quite uniform. With gaspers on and off, the vertical temperature variation at a given seat did not exceed 2.8 $^{o}$C, and the horizontal temperature variation across a row did not exceed 4.4 $^{o}$C, which met the requirements of ASHRAE Standard 161 (2007). Higher temperature variation may cause substantial difference in thermal sensation of passengers and may lead to thermal discomfort in the cabin.

Figure 9 compares the air velocity distributions at the three longitudinal sections of the cabin with the gaspers off and on. When the gaspers were off, the jet from the main diffusers was not very strong by the time it reached seat C. The thermal plume generated by the manikin in seat C may have been stronger than the jet. As a result, at section ASLC the airflow direction was primarily upward. On the other hand, when the gaspers above seat C were turned on, the jets from the gaspers were much stronger than the thermal plumes from the manikins. Therefore, in the lower part of section ASLC the air primarily flowed downward. In the aisle (section CALS), the flow in the vertical direction was similar to that in section ASLC. In the longitudinal direction, however, the flow direction in the lower part of section CALS was almost the opposite of that when the gaspers were off. These observations indicate a very complex three-dimensional airflow pattern. In the longitudinal section through the window seats (WSLS), the flow direction was mainly upward because of thermal buoyancy, regardless of whether the gaspers were on or off. This was because the section was located in the entrainment region of the jets.

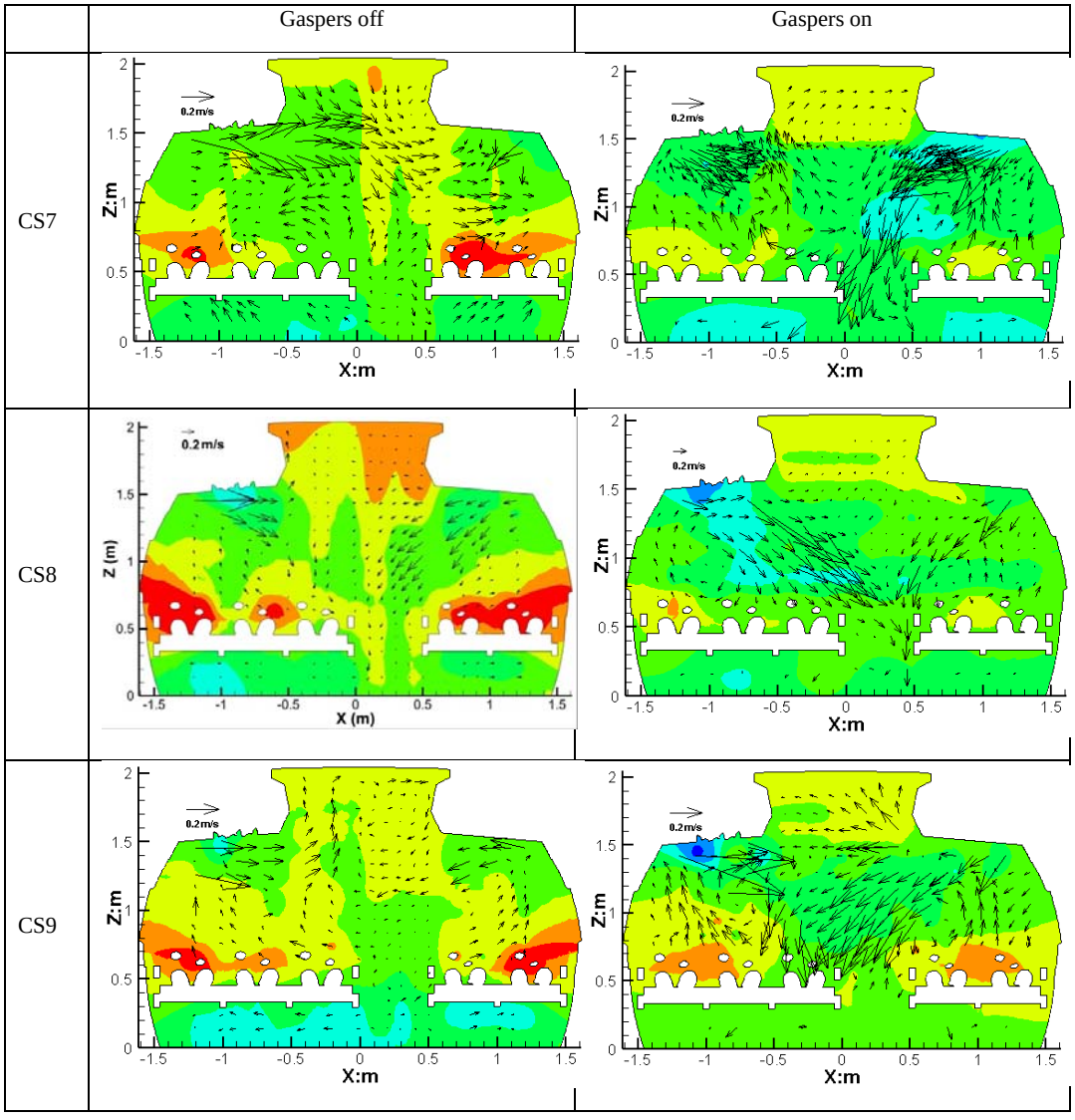

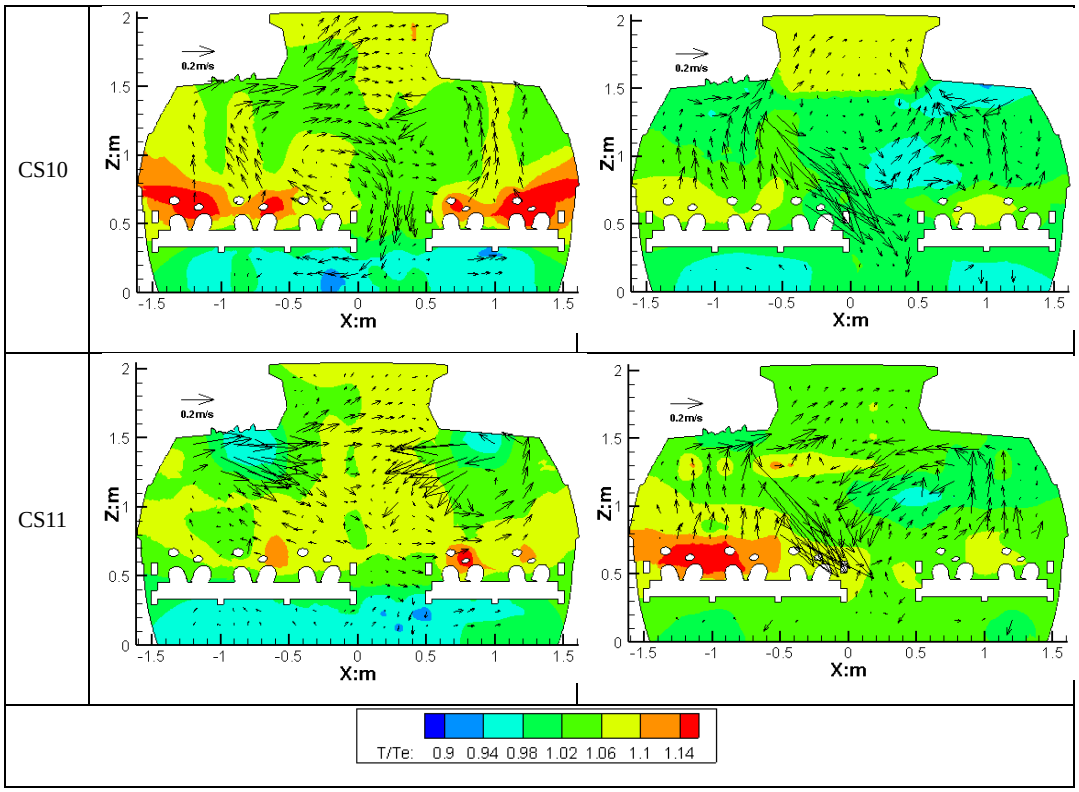


*Figure 8. Comparison of the air velocity vectors and temperature distributions at the five cross sections in the occupied economy-class cabin with gaspers off and on. The air temperature (T) was normalized by the mean air temperature at the exhaust outlets (Te). (The white areas in the figure were manikins' body parts and seat components in the section).*

The air temperature distributions in the three longitudinal sections exhibited some stratification. In sections ASLS and CALS, the relatively low air temperature in the lower part of the cabin was mainly caused by the cool jets from the diffusers and gaspers. When the gaspers were on, the air temperature in the aisle was lower than that when the gaspers were off. This difference is understandable because the air from the gaspers was cooler than the mean air temperature in the cabin, and the jets from the gaspers were all directed towards the aisle. In section ASLS, the air at seat A circulated at waist height because of the jets from the main diffusers. Thus, the air temperature in this region may have been higher than in other parts of the longitudinal section. Although the airflow pattern with the gaspers on was somewhat different from that with the gaspers off, the temperature distributions did not differ very much, which indicates very good mixing conditions in the cabin.

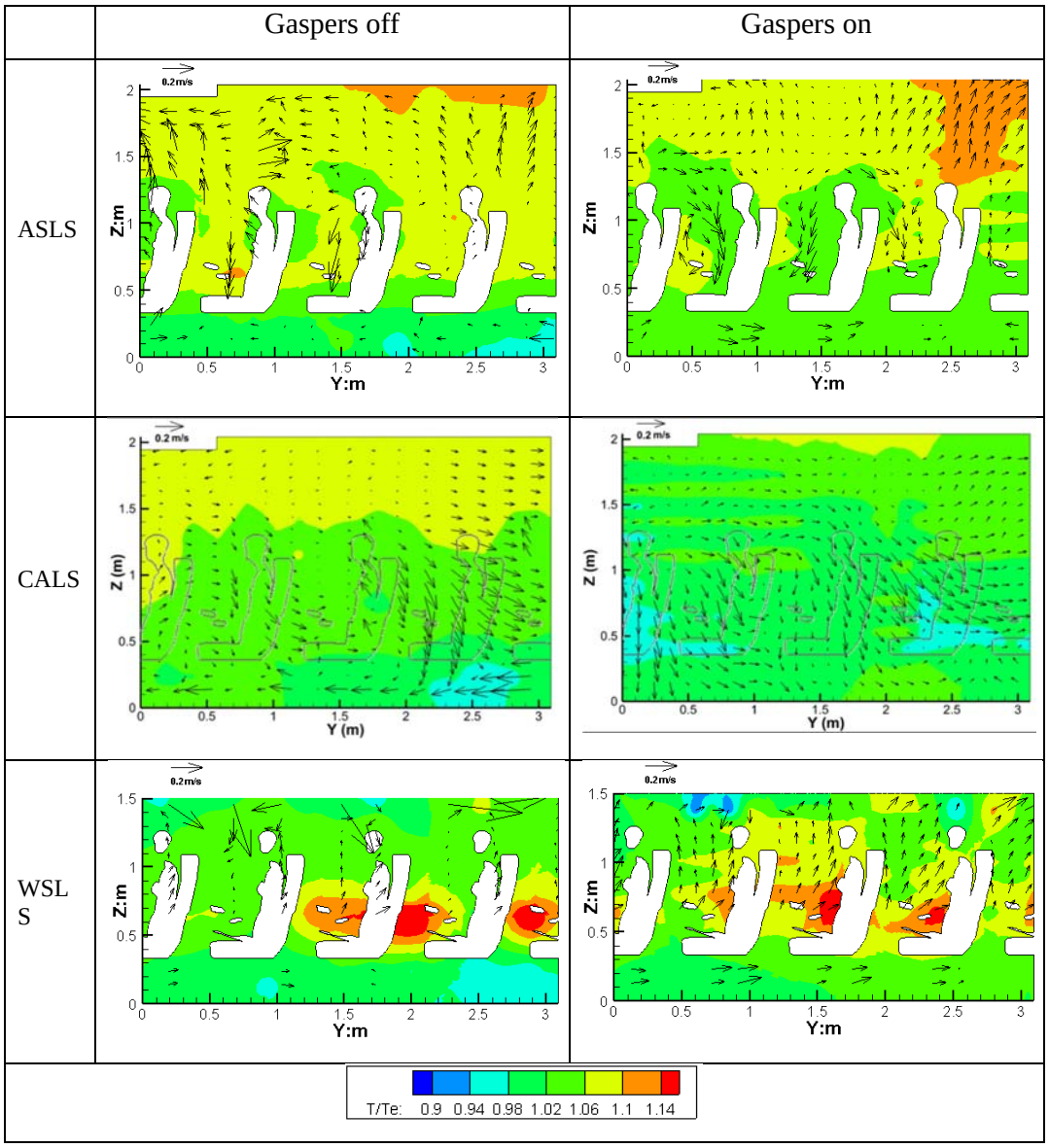


*Figure 9. Comparison of the air velocity vectors and temperature distributions at three longitudinal sections in the occupied economy-class cabin with gaspers off and on. The air temperature (T) was normalized by the mean air temperature at the exhaust outlets (Te). The white areas in the figure were manikins' body parts and seat components in the section).*

**Contaminant concentration distributions with gaspers on and off**

This study used $SF_6$ to simulate a gaseous contaminant. Figure 10 shows the measured $SF_6$ distributions with gaspers off and on at five cross sections (CS7, CS8, CS9, CS10, and CS11) in the fully occupied economy-class cabin. The concentration distribution in all five cross sections changed significantly when the gaspers were turned on. The gaspers were able to push a large amount of $SF_6$ from the source location to the lower region of the cabin. When the gaspers were off, the $SF_6$ concentration was high in the upper region of the cabin because the contaminant was moved upward by the thermal buoyancy from the manikins. Even though

the gaspers supplied fresh air to the cabin, it was possible for the $SF_6$ concentration in the breathing zone to be higher when the gaspers were on than when they were off.

When the gaspers at the C seats were turned on, a high $SF_6$ concentration was observed above the D and E seats because of the air recirculation in the area. In the head regions of the C seats, however, the $SF_6$ concentration was low because of the fresh air supply from the gaspers. The $SF_6$ concentration was generally higher on the left side of the cabin than on the right side because of the jets from the gaspers above the B seats.

Figure 11 shows the measured $SF_6$ distributions in the three longitudinal sections when the $SF_6$ source was located at seat 9C. When the gaspers were off, the direction of the longitudinal flow was generally toward the front of the cabin, and therefore the $SF_6$ concentration was high at the front. In the upper part of the cabin, the concentration was high because of thermal buoyancy from the heated manikins. When the gaspers were turned on, the longitudinal flow changed direction because the jets from the gaspers were directed downward toward the rear. Therefore, the $SF_6$ concentration was high at the rear of the cabin. The jet could also form a local re-circulation pattern and cause a high concentration of $SF_6$ at the mid-height of the cabin. Because only a small amount of fresh air was injected into the cabin from the gaspers, the jets did not provided cleaner air in the breathing zone to dilute the high concentration. The high air speed from the gasper induced a large amount of cabin into the jet growth. This pushed down the contaminant to the lower part of the cabin.

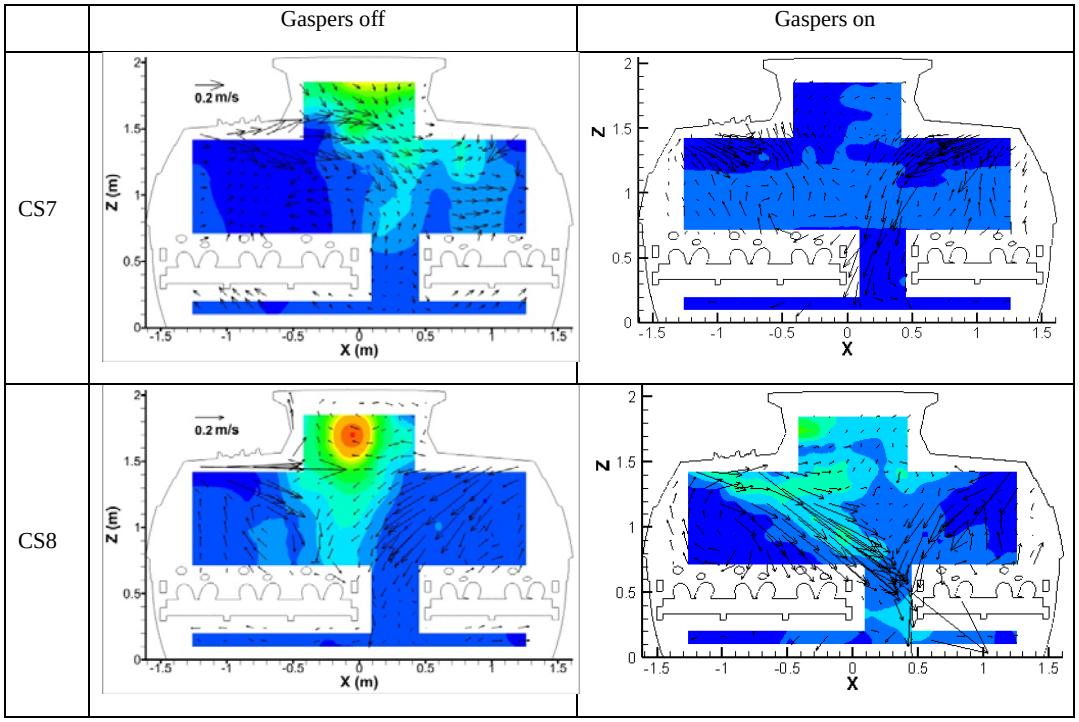

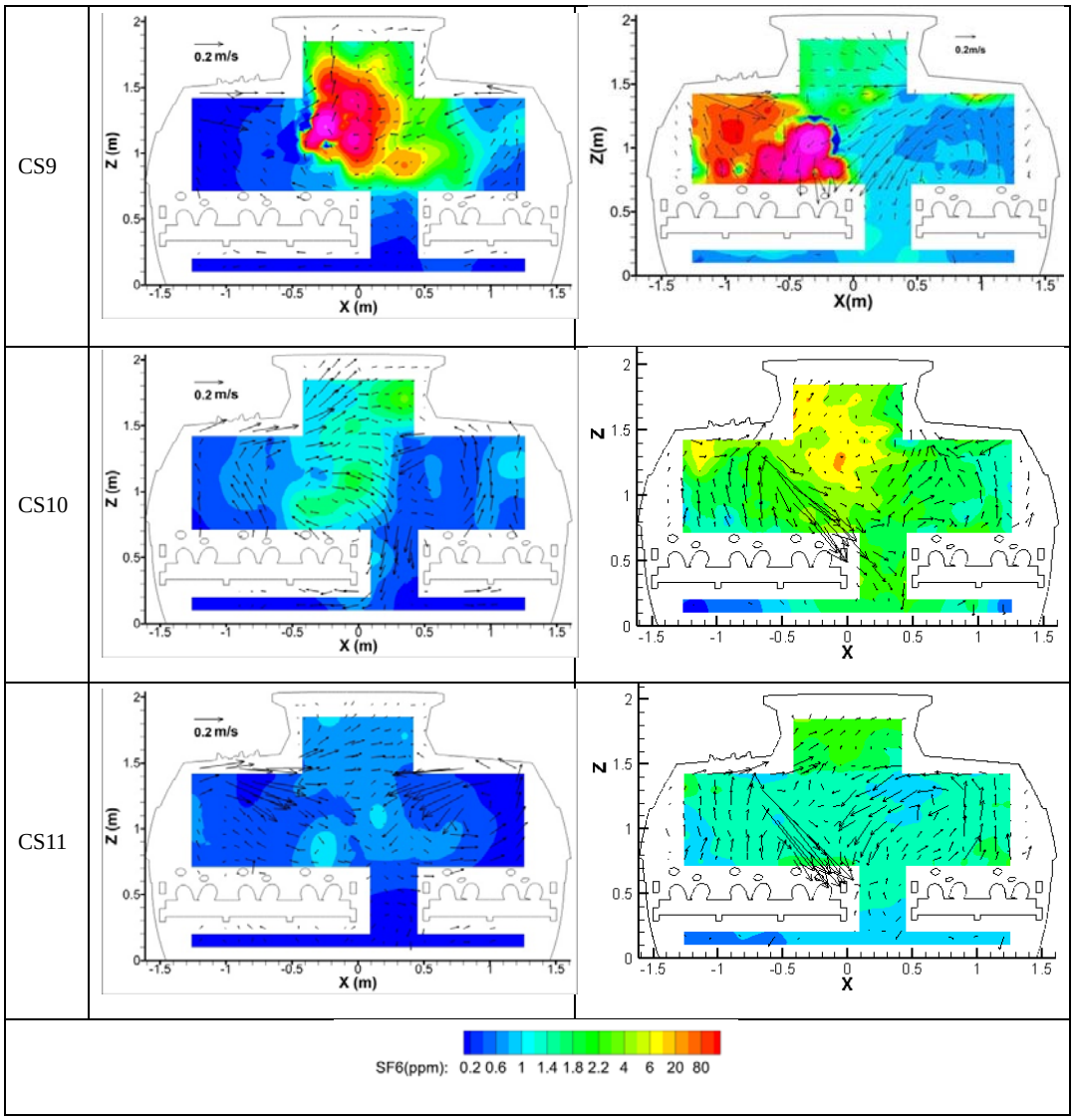


*Figure 10. Comparison of the air velocity vectors and $SF_6$ distributions at the five cross sections in the occupied economy-class cabin with gaspers off and on.*

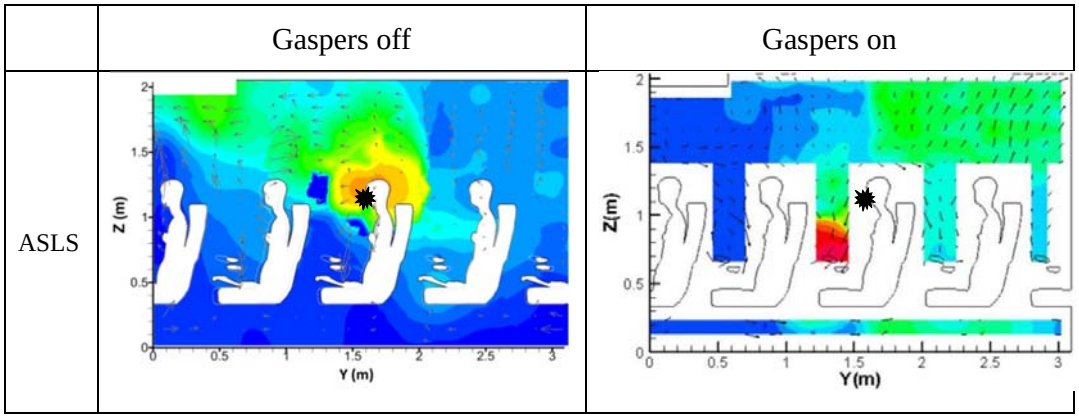

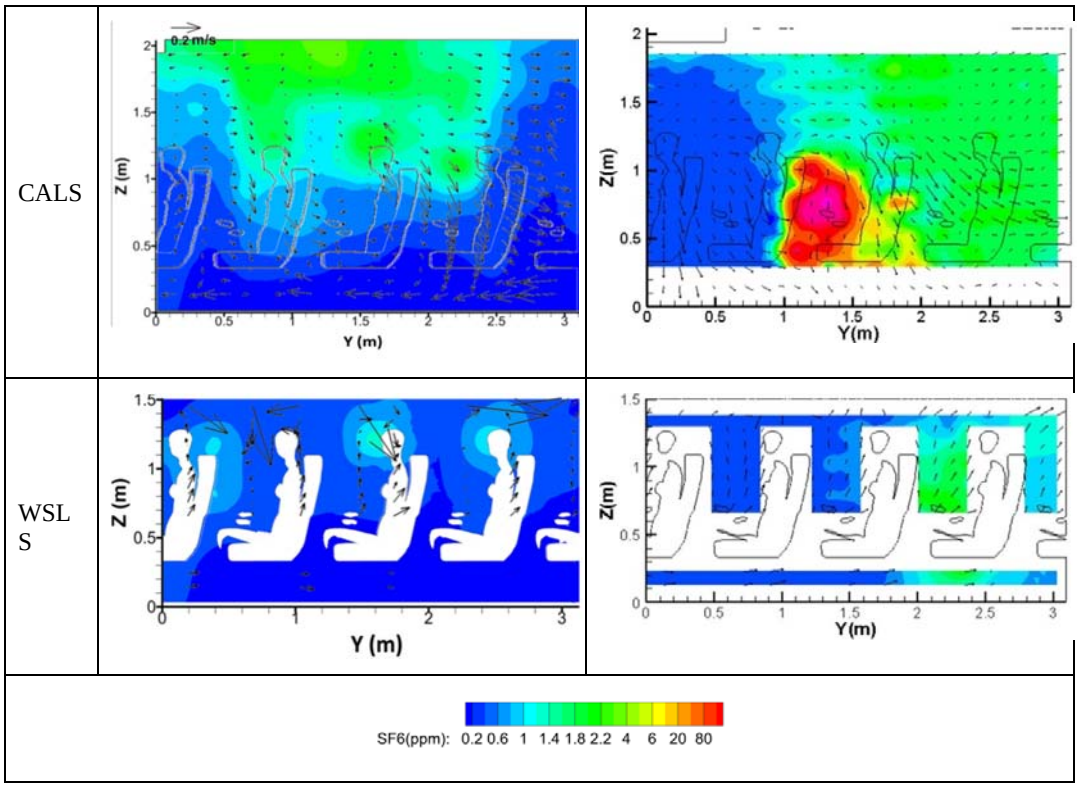


*Figure 11. Measured $SF_6$ concentration distributions in the three longitudinal sections in the occupied economy-class cabin with gaspers off and on.*

**Contaminant concentration distributions with sources in different locations**

This study also investigated the impact of source location on contaminant distribution in the MD-82 cabin when the gaspers were on. An $SF_6$ source was placed in the breathing zones above seats 9A, 9C, and 9E, in turn. The $SF_6$ concentration distributions were measured at breathing level between rows 7 and 11as shown in Figure 12. Since air was supplied on both sides of the cabin in the "shoulder" areas, the general airflow pattern in a cross section contained two large circulations, as illustrated in Figures 8 and 10. Because of this airflow pattern, the $SF_6$ was contained within the region around the source. Thus, when the source was at seats 9C and 9E, the $SF_6$ concentration was high on the left side of the cabin. When the source was at seat 9A, the concentration was high on the right side of the cabin. The high concentration at seat 9C may have been due to the seat's location near the middle of the cabin, where two air supply jets merged.

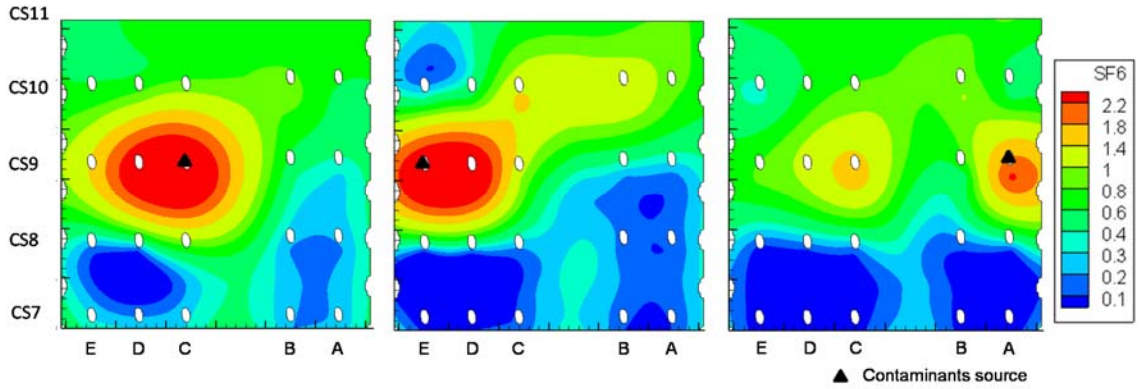


*Figure 12. $SF_6$ concentration distributions at breathing level with the source location at seats 9E (left), 9C (middle), and 9A (right).*

Figure 11 shows that the longitudinal flow was directed towards the back of the cabin due to the jet effect. Thus, the SF6 concentration in the rear section was higher than in the front section, regardless of which seats the contaminant source was located in.

## Discussion

### Impact of the robot system on experimental speed and accuracy

To minimize disturbance of the airflow pattern by the operators and to increase the precision of sensor positioning during the experiment, this investigation used a three-dimensional robot system. In our previous study, the sensors were moved from one position to another manually (Liu et al., 2012). The operators had to enter the cabin, and their movements disturbed the airflow. A period of 10 minutes was needed for the flow to return to its original stable condition. In the present study, the three-dimensional robot system traveled at a very slow speed of 10 mm/s, and the airflow became stable again within one minute after the sensors had been positioned. The use of the robot system increased the speed of our measurements. The movement resolution of the robot in all three directions was ±0.5 mm, which was much more accurate than manual placement of the sensors by the operators. Figure 13 shows the averaged air velocity and the confidence intervals of the air velocity, measured with and without the presence of the robot system at several locations in the breathing zone and along the vertical direction in the aisle. The two sets of air velocity data are very close to each other. A paired T-test showed no significant differences between the two sets of data. Since the robot system was more accurate in placing the anemometers, the data obtained in this manner should be better.

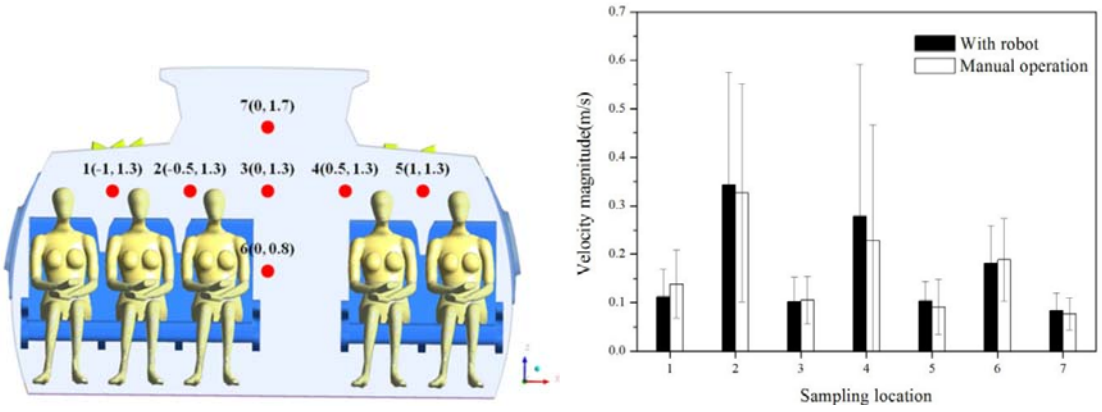


(a) (b)

*Figure 13. (a) Measurement positions for air velocity and (b) comparison of the 10-minute-averaged velocities at these positions when the sensors were placed manually and by the robot system.*

## Airflow from the gaspers

Air is typically supplied to an economy-class cabin at a rate of 10 L/s per passenger. In the current study, the airflow rate from each semi-opened gasper was 0.66±0.03 L/s. When the gaspers are opened to the maximum possible degree, the airflow rate per gasper increases to 1.65 L/s, or 16.5% of the total ventilation rate. In this study, only two gaspers per row were turned on, and thus the total flow rate from the gaspers was only 2.2% of that supplied to the cabin. Although the amount of air flowing from the gaspers was small, its impact on the air velocity and $SF_6$ concentration distributions in the cabin was substantial, as shown in Figures 8 through 12, by comparing with those without gaspers on as reported by Liu et al. (2012).

It is also interesting to observe the air velocity decay along the axial jet direction of a gasper, as shown in Figure 14. The jet from the gasper decayed gradually. At a distance of 90 mm from the gasper outlet, the rate of decay decreased. The flow from a gasper can be regarded as the jet from a nozzle with a circular cross-section, in which the velocity decay can be calculated by (Cai and Long, 2009):

$$V_m/V_0=0.48/(as/d_0+0.147) \quad (1)$$

where $V_m$ is the maximum axial velocity of the jet (m/s), $V_0$ is the air velocity at the outlet (m/s), $s$ is the distance from the outlet along the axial direction (m), $d_0$ is the outlet diameter (m), and $a$ is a coefficient.

Figure 14 compares the measured velocity distribution along the axial direction of the jet with that calculated by Eq. (1). The results show that the velocity of the air flowing from the gasper was greater than 40 m/s at the core very close to the gasper outlet, and it decayed rapidly

along the radial direction. Eq. (1) provides an accurate prediction of the velocity decay of the jet. Therefore, it can be concluded that the jet from the gasper corresponds to that of a round jet. More information about the turbulence intensity and velocity development can be found in Dai et al. (2014). When CFD simulations are used to study a personalized ventilation system, the jet from a gasper can be reduced to that from a round jet. The use of the jet equation would greatly reduce the meshes needed for the complex gasper geometry so that the computing speed can be enhanced and computer capacity can be reduced.

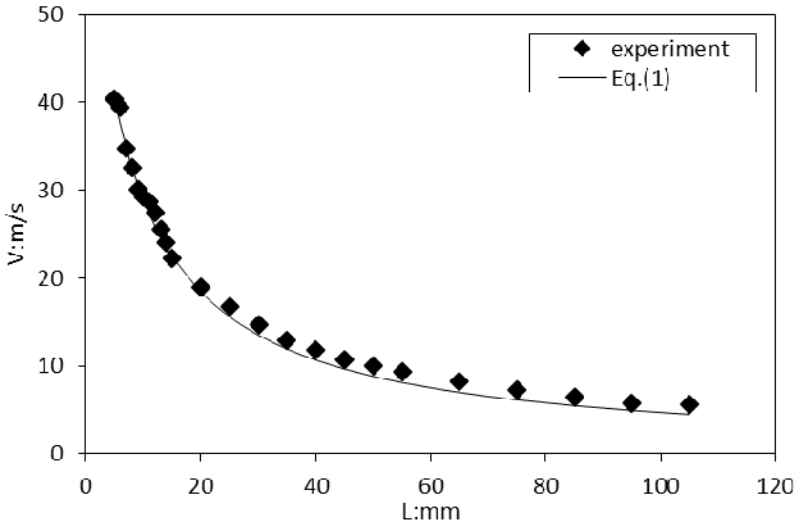


*Figure 14. Comparison of the decay in air velocity from a gasper as measured by a hot-wire anemometer with that calculated by Eq. (1).*

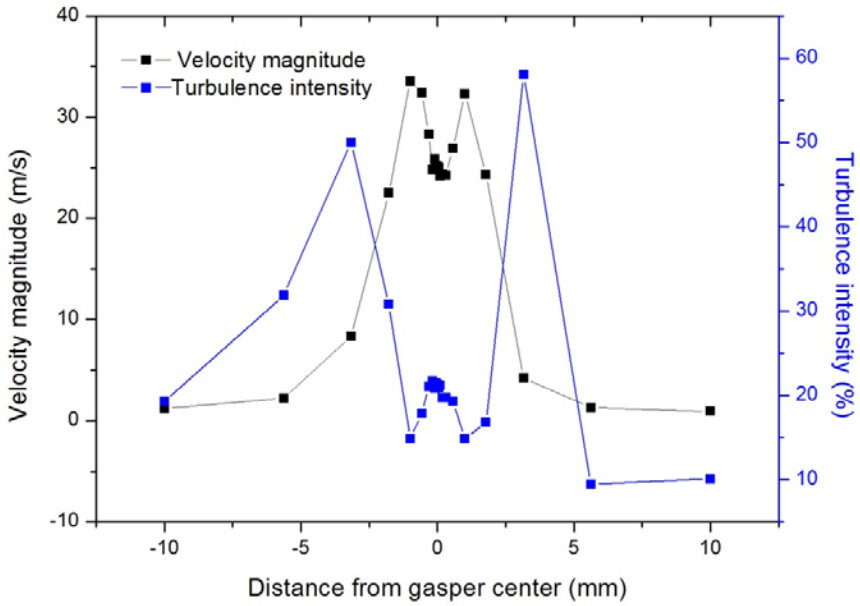


*Figure 15. Distribution of measured velocity and turbulence at a gasper inlet*

Figure 15 shows the distribution of the measured air velocity and turbulence at the gasper inlet. The measurement position was around 10 mm from the outlet. As seen from the figure, the velocity exhibited two peaks at the gasper center, and decreased with the distance away from the center. The velocity profile was similar with the one in the literature by Dai et al. (2014). The turbulence intensity showed the opposite trend with the velocity, especially close to the core. However, the velocity was large at the center with an average of 28 m/s. The velocity fluctuation was small with a turbulence intensity of 17%.

**Suggestion for CFD validation**

Although this paper provides a lot of information, it is insufficient for someone to use it for CFD validation. Interested readers can contact corresponding author for detailed information on thermos-fluid boundary conditions and the air distributions. When simulating such a flow, the data on CS7 and CS11 can be used as the boundary conditions on the two ends. The data at CS8, CS9, and CS10 can be used for validating the corresponding CFD results. As for the experimental accuracy, please refer to the discussion on Liu et al. (2012).

**The momentum fluxes in the cabin**

In the cabin, with the gaspers on, the velocity was generated by three momentum sources: the air diffuser, gaspers and the thermal plumes from the heated manikins These sources could partly compete with each other. Therefore it is important to quantify the relative strength of each source. The strength was quantified by the specific momentum flux, which were calculated by the flow rate times the supply velocity. Table 1 listed the strengths of the momentum sources. The flow rate from the gaspers was much smaller than that from air diffusers so that the effect on diluting the $SF_6$ concentrations around the passengers was small. However, the effect of gaspers on the air motions was much larger because the momentum flux was far higher than that from the air diffusers, which can be observed from Figure 10. Table 1 compares the momentum flux from the heated manikins with that from the air diffusers. The two forces were comparable indicating that both of them were important to the airflow and concentration fields.

*Table 1. Momentum fluxes from the air diffuser, gaspers and thermal plumes from the heated manikins in each row of the cabin*

| Momentum sources | Specific momentum flux ($m^4/s^2$) | Averaged velocity (m/s) | Equivalent flow rate ($m^3/s$) |
|---|---|---|---|
| Air diffuser* | 0.045 | 1.42 | 0.032 |
| Gaspers | 38.28 | 29 | $1.32\times10^{-3}$ |
| Heated manikins** | 0.074 | 0.38 | 0.195 |

* The flow rate and velocity at diffuser can be found in Liu et al. (2012).

[**]The specific momentum flux was calculated by assuming heat manikins as line heat sources by the equations in Enai, et al. (1987).

## Conclusion

This paper presented the distributions of air velocity, air temperature, and contaminant concentration measured in an MD-82 air cabin when two of five gaspers close to the aisle in each row seats were turned on. The results from our previous study with all the gaspers off (Liu et al. 2012) were used for comparison. Gasper operation can have a substantial impact on the local and global distributions of air velocity, air temperature, and contaminant concentration. The present study has led to the following conclusions:

- The jets from the gaspers were very strong. The jets greatly increased the air velocity in the cabin, even though the total flow rate from the gaspers was only 2.2% of the overall air supply to the cabin. The jets were able to penetrate the thermal plumes formed by the heated manikins, and they formed strong air recirculation patterns in the cabin.
- When the gaspers were on, the jets from the gaspers enhanced the mixing of air, and thus the air temperature in the cabin was slightly more uniform than when the gaspers were off.
- Since the jets from the gaspers were directed towards the back, the gaseous contaminant was blown to the rear section of the cabin. Because only a small amount of fresh air entered through the gaspers, the jets did not provided cleaner air in the breathing zone. Instead, the contaminant was pushed down to the lower part of the cabin.
- The air velocity decay along the axial direction of the jet from a gasper was calculated by using the equation for a nozzle.

## Acknowledgment

The authors are grateful for the financial support of this research by the NSFC (Grant No.51408413), National Basic Research Program of China (the 973 Program) through Grant No. 2012CB720100 and the Center for Cabin Air Reformative Environment (CARE) at Tianjin University, China.

## References

Anderson D. M. (2012), Effect of Gaspers on Airflow Patterns and the Transmission of Airborne Contaminants within an Aircraft Cabin Environment, *Master thesis Kansas State*

*University*.

ASHRAE (2007) *Air Quality within Commercial Aircraft*, Atlanta, GA, American Society of Heating, Refrigerating and Air Conditioning Engineers (ASHRAE Standard 161-2007).

Bosbach, J., Pennecot, J., Wagner, C., Raffel, M., Lerche, T., Repp, S. (2006) Experimental and numerical simulations of turbulent ventilation in aircraft cabins, *Energy*, **5**, 694-705.

Cai, Z., Long, T. (2009) Hydrodynamics of pumps and fans, Beijing, *China Building Industry Press*. (In Chinese)

Chao, C., Wan, M., Law, A. (2004) Ventilation performance measurement using constant concentration dosing strategy, *Building and Environment*, 11, 1277-1288.

Dai, S., Sun H., Liu W., Guo Y., Jiang N., Liu J. (2015). Experimental study on characteristics of the jet flow from an aircraft gasper. *Building and Environment* 93, Part 2: 278-284.

Enai, M. (1987) A feasibility study on open cooling- the characteristics of buoyant ventilation through high side openings, *Proceeding of international conference on air distribution in ventilation space in Roomvent (session A), Stockholm, June 1987*.

Etheridge, D., Sandberg, M. (1996) Building ventilation: Theory and measurement, *Chichester, John Wiley & Sons*.

Haghighat, F., Allard, F., Megri, A. C., Blondeau, P., Shimotakahara, R. (1999) Measurement of thermal comfort and indoor air quality aboard 43 flights on commercial airlines, *Indoor and Built Environment*, **1**, 58-66.

Huang, Y., Shen X., Li J., Li B., Duan R., Lin C.-H., Liu J., Chen Q. (2015). A method to optimize sampling locations for measuring indoor air distributions. *Atmospheric Environment* **102**: 355-365.

Kühn, M., Bosbach, J., Wagner, C. (2009) Experimental parametric study of forced and mixed convection in a passenger aircraft cabin mock-up, *Building and Environment*, **5**, 961-970.

Li, F., Liu, J., Pei, J., Lin, C-H, Chen, Q. (2014) Experimental study of gaseous and particulate contaminants distribution in an aircraft cabin, *Atmospheric Environment*, **5**, 223-233.

Li, R., Sekhar, S., Melikov, A. K. (2010) Thermal comfort and IAQ assessment of under-floor air distribution system integrated with personalized ventilation in hot and humid climate, *Building and Environment*, **9**, 1906-1913.

Lin, C.,Wu, T., Horstman, R., Lebbin, P., Hosni, M., Jones, B., et al. (2006) Comparison of large eddy simulation predictions with particle image velocimetry data for the airflow in a generic cabin model, *HVAC&R Research*, **3c**, 935-951.

Liu, W., Wen, J., Chao, J., Yin, W., Shen, C., Lai, D., et al. (2012) Accurate and high-resolution boundary conditions and flow fields in the first-class cabin of an MD-82 commercial airliner, *Atmospheric Environment*, **6**, 33-44.

Melikov, A. K., Cermak, R., Majer, M. (2002) Personalized ventilation: Evaluation of different air terminal devices, *Energy and Buildings*, **8**, 829-836.

Niu, J., Gao, N., Phoebe, M., Huigang Z. (2007) Experimental study on a chair-based personalized ventilation system, *Building and Environment*, **2**, 913-925.

Wang, A., Zhang, Y., Sun, Y., Wang, X. (2008) Experimental study of ventilation effectiveness and air velocity distribution in an aircraft cabin, *Building and Environment*, **3**, 337-343.

Wisthaler, A., Strøm, T. P., Fang, L., Arnaud, T. J., Hansel, A., MÄrk, T. D., et al. (2007) PTR-MS assessment of photocatalytic and sorption-based purification of recirculated cabin air during simulated 7-h flights with high passenger density, *Environmental Science & Technology*, **1**, 229-234.

Yan, W., Zhang, Y., Sun, Y., Li, D. (2009) Experimental and CFD study of unsteady airborne pollutant transport within an aircraft cabin mock-up, *Building and Environment*, **1**, 34-43.

Zhang, T., Li, P., Wang, S. (2012) A personal air distribution system with air terminals embedded in chair armrests on commercial airplanes, *Building and Environment*, **47**, 89-99.

Zhang T., Tian L., Lin C.-H., Wang, S. (2012). Insulation of commercial aircraft with an air stream barrier along fuselage. *Building and Environment* ,**57**: 97-109.

Zhang, Z., Chen, X., Mazumumdar, S., Zhang, T., Chen, Q. (2009) Experiment and numerical investigation of airflow and contaminant transport in an airliner cabin mockup, *Building and Environment*, **1**, 85-94.